
Finite Element Analysis of Folds

O. Stephansson

Phil. Trans. R. Soc. Lond. A 1976 **283**, 153-161

doi: 10.1098/rsta.1976.0075

Email alerting service

Receive free email alerts when new articles cite this article - sign up in the box at the top right-hand corner of the article or click [here](#)

Finite element analysis of folds

BY O. STEPHANSSON

Department of Rock Mechanics, University of Luleå, Luleå, Sweden

Finite element analysis of the time-dependent deformations of layered viscous solids serves as the basis of the study of the mechanics of folding. The progressive development of folds by buckling in single and multilayer models compressed parallel to the layering is reviewed. Fold geometries are shown to vary from parallel, for large viscous contrasts, to nearly similar, for low contrasts. For models with the same viscosity contrast the geometry depends upon the wavelength/thickness ratio, so that thin-layer folds behave in the most 'competent' fashion with a great amount of buckle shortening.

The development of stresses around folds is discussed. As the fold grows the principal stresses rotate and the magnitude changes quite drastically for models with high viscosity contrast. These folds also have the gradient of mean stress directed perpendicular to the layer in the hinge part of the competent layer. The heterogeneous stress distribution, as it appears in a fold structure, generates a free energy gradient, and diffusion current will tend to bring the system to a state of equilibrium by one or more of the following events: (1) introduction of new mineral species; (2) polymorphic phase changes; (3) a change in chemical composition and (4) a change in grain size.

Future development of the finite element analysis of folding is discussed.

INTRODUCTION

One of the chief objectives of structural geology is the study of the mechanics of the past and present motion of matter in the Earth's crust. In the case of many geological structures, it would be desirable to study the relationships between the present observed geometries, their initial form, and the stress distribution under which they developed. The development of digital computers has made possible the use of numerical computer-based methods to solve complex continuum problems. One of them, the finite element method, is a general method of structural analysis, in which a continuum or continuous structure is replaced by a finite number of elements interconnected at a finite number of nodal points. The method can be used to determine the displacement of the nodal points, and the stresses within the elements developed in two- or three-dimensional models of arbitrary geometry and material property.

The basic understanding of the mechanism of fold formation came from the theoretical analyses of viscous buckling made by Biot (1961, 1965) and Ramberg (1961, 1964). Their work concerns only the instantaneous development of folds from initial irregularities in the layers, which can be considered to be the sum of a harmonic series of sine and cosine waves of different wavelengths and amplitudes. One assumption of the theory is that the amplitudes of the initial sinusoidal waves or components of an harmonic series must be small, and that a dominant wavelength is most likely to appear in a given system. This dominant wavelength, being that of the sinusoidal wave which is initially amplified the most, has been used as a starting situation for most of the finite-element analysis of buckling folds, e.g. Dieterich & Carter (1969), Stephansson & Berner (1971), Hudleston & Stephansson (1973), Stephansson (1974). This

paper examines the changes in fold shape, strain, and various parameters of stress including principal, deviatoric, shear and mean stresses in folded models produced by finite-element analysis.

FOLD-SHAPE DEVELOPMENT

Dieterich & Carter (1969) and Dieterich (1969) studied the development of folds to large amplitudes in viscous layers set in a less viscous medium by the application of finite-element analysis. This was the first application of the method to problems in structural geology. Computations were made with viscosity contrasts of 42/1 and 17.5/1 between the competent layer and the matrix. Finite strain and stress fields were derived throughout the folding history for folds in layers which were initially in the form of low-amplitude sine waves at the dominant wavelength/thickness ratio. Layer shortening occurred in the early stages of folding and was greatest in the case of the lower viscosity contrast. At the higher viscosity contrast, 42/1, very slight variations in thickness with dip were detectable at high amplitudes. At the lower viscosity contrast very pronounced thickening in the hinges, and thinning in the limbs of the folds were apparent. The model material used in this study was a linearly viscous fluid.

Parrish (1973) extended the linear model to a nonlinear one, and folded a viscous layer according to a nonlinear flow law of the form

$$\dot{\epsilon} = A \exp(-Q/RT)\sigma^n,$$

where $\dot{\epsilon}$ is the strain rate, A , n , material constants, Q , activation energy for creep, R , gas constant, T , temperature and σ , difference between maximum and minimum compressive stresses. The creep law is in agreement with the experimental results of rock deformation. The fold model had a wavelength of thickness ratio of 9:1, which is slightly greater than the 8:1 ratio predicted by the theoretical formula for buckling instability using the viscosity contrast of 12. The resulting fold geometry resembles the linear models in that a broad open concentric geometry developed, which is due to the fact that the power law increased flow in the inner hinge and decreased flow in the outer hinge. The overall thickness of the layer increases by 35% of its original thickness during the deformation of 90% shortening.

Hudleston & Stephansson (1973) studied three single-layer models for a viscosity contrast between layer and matrix given by $\mu_1/\mu_2 = 10$, where μ_1 is the viscosity of the layer. In one model the wavelength/thickness ratio, L/h , was 7.4, as predicted for the dominant folds at this viscosity contrast by the theoretical expression of Biot (1961) and Ramberg (1961). In the other two models the L/h ratios were taken as 4.0 and 15.1. The progressive growth of the fold shows that the geometry depends upon the L/h ratio so that flattening dominates the thick-layer model, whereas a large amount of buckle shortening accompanies the deformation of the thin layer. This is illustrated in figure 1, where the changes in limb dip, amplitude and arc-length with total shortening in the three models are recorded curves A, B, C. It is apparent from figure 1 that the thin-layer fold has behaved in the most 'competent' fashion and the thick-layer fold in the least 'competent'.

The progressive growth of folds with viscosity contrasts given by $\mu_1/\mu_2 = 10, 100$ and 1000 are shown in figure 2. For the models with the contrast 100 and 1000 the folds maintain an almost parallel shape, and follow a path of development similar to that traced by the dominant wavelength folds in a numerical study made by Chapple (1968). Folds developed in slightly compressible material show a slight thinning in the hinge regions. This was demonstrated in the finite-element analysis of a multilayer fold model by Stephansson & Berner (1971).

Summarizing the results of foldshape development from the finite element models, layer shortening dominates in the early stages of folding and is greatest in the case of low viscosity contrast. Low viscosity contrast emphasizes thickening in the hinges and thinning in the limbs. For models with the same viscosity contrast the geometry depends upon the wavelength/thickness ratio so that flattening dominates the thick layer model. For models with high viscosity contrast the folds maintain an almost parallel shape with small deviations depending upon the compressibility of the material. Finally, the fold geometry and configuration of the strain field are affected somewhat by the choice of the initial amplitude.

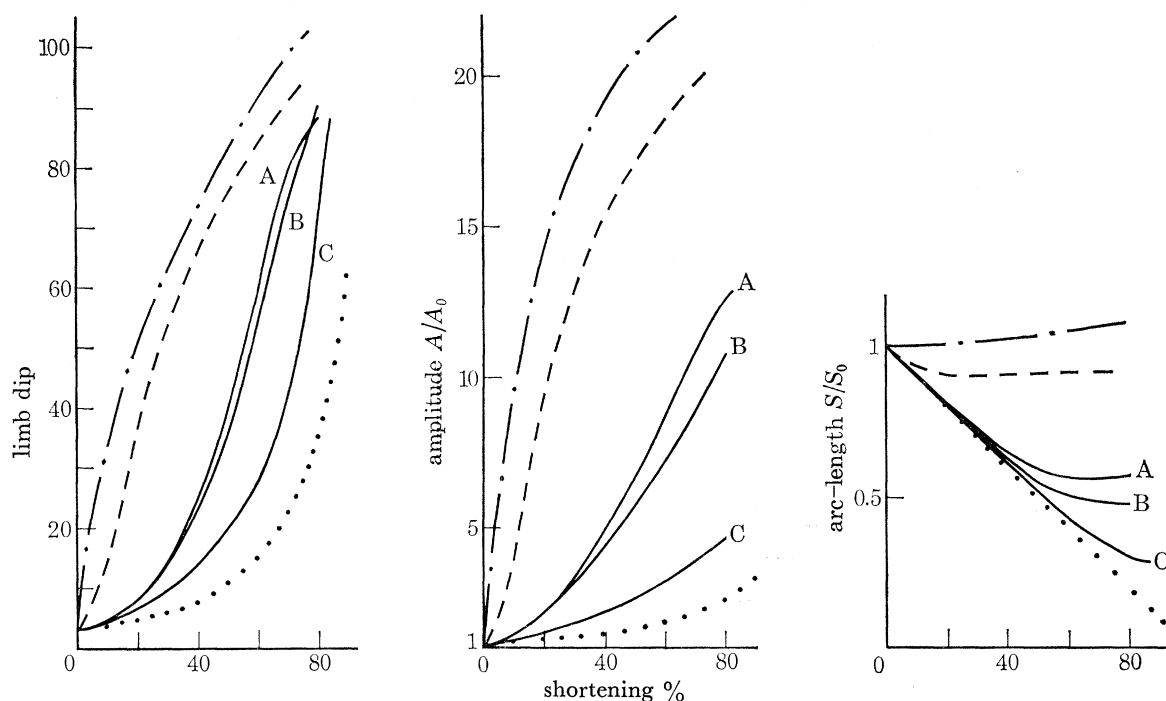


FIGURE 1. Changes of limb dip, amplitude and arc-length, with overall shortening for finite element models at different viscosity contrasts and wavelength/thickness ratios. A_0 and S_0 are the initial amplitude and arc-length. After Hudleston & Stephansson (1973).

	μ_1/μ_2	λ/h
— · — · —	1000	34.6
— — —	100	16.0
— — —	10	A 15.1
— — —	10	B 7.4
— — —	10	C 4.0
.....	1	3.46

Dieterich (1969) studied the possible relation between the orientation or geometry of axial-plane foliation, and the orientation of stress and finite strain in the vicinity of folds. He found that the directions perpendicular to ϵ_1 , the maximum principal component of compressive strain, in the model closely coincide with the natural cleavage pattern throughout the model. The fanning and refraction of the minimum principal component of compressive strain, ϵ_3 , in the matrix and folded layer were considerably weaker for models with a lower contrast in viscosity. It is therefore concluded that axial-plane foliations in nearly concentric folds form in response to total strain, and develop perpendicular to the directions of maximum total shortening.

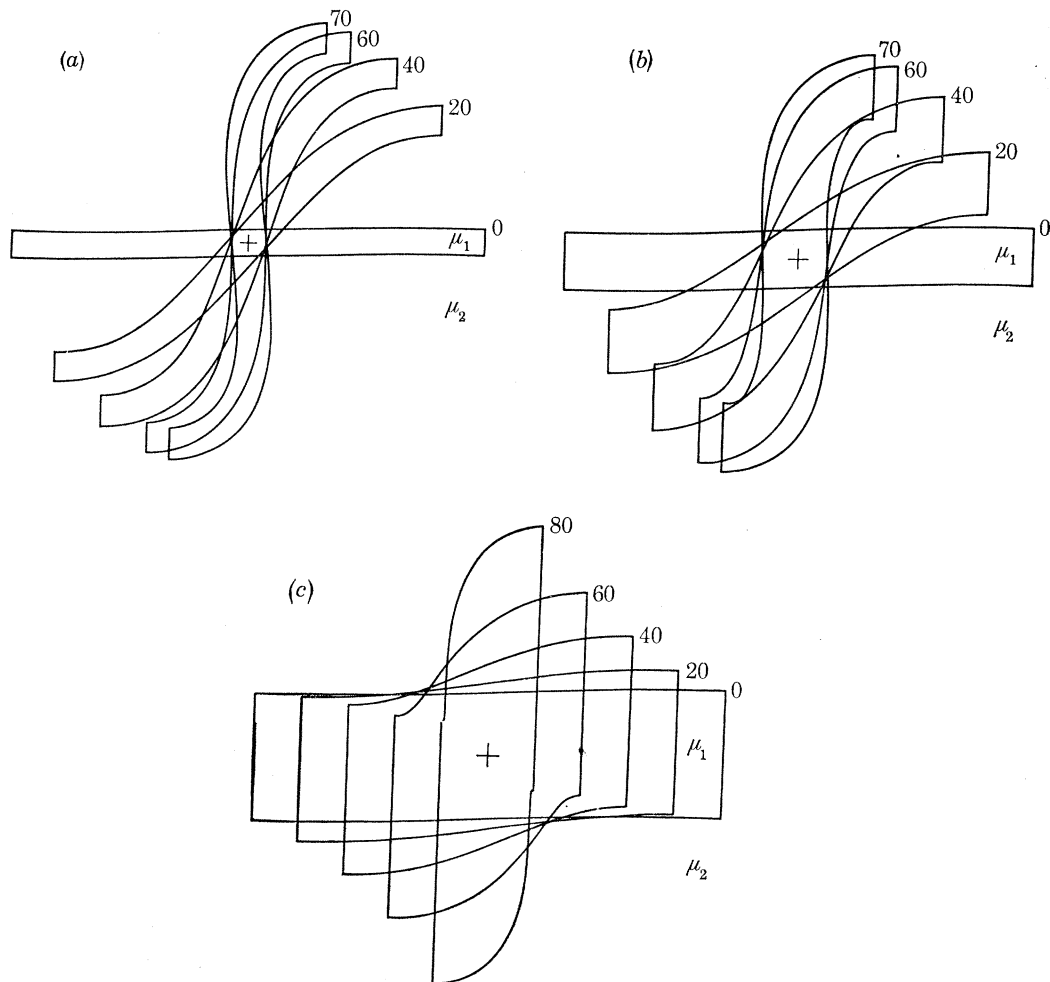


FIGURE 2. Single-layer buckle folds produced by finite element analysis. Layer parallel shortening increases with decreasing viscosity contrast.

	μ_1/μ_2	λ/h
<i>a</i>	1000	34.6
<i>b</i>	100	16.0
<i>c</i>	10	7.4

PRINCIPAL STRESSES AROUND FOLDS

The geometry of folds and the distribution of stresses are found from each of the strain increments during modelling. For models with a large viscosity contrast, the principal compressive stresses within the competent layer are initially oriented parallel to the layer and are of uniformly large magnitude. As the fold grows, the principal stresses rotate to larger angles to the layer and the magnitude changes quite drastically. In the limbs of the folded layer the maximum principal stress rotates to larger angles to the layer. After a certain amount of total strain at about 15% for the layer with the viscosity contrast of 42, the principal stresses change in the outermost portion of the fold hinge, where the extension parallel to the layer causes the principal compressive stress to become oriented normal to the layer. Along the inner portion of the fold hinge the principal compressive stress is of large magnitude, and remains almost parallel

to the layer during the folding. For models with a slight viscosity contrast the stresses remain nearly parallel to the direction of compression throughout the folding. The stress differences between layer and matrix are of the same magnitude as the viscosity contrast. According to Dieterich & Carter (1969) there is no region of relative tension along the outer portion of the hinge if the viscosity contrast is 5 to 1 or less. The stress distribution in the nonlinear finite element fold model of Parrish (1973) is similar to the linear models.

Finite element analysis of multilayer fold systems by Stephansson & Berner (1971) indicated great differences in stress distribution between folds produced in compressible and incompressible material. The orientation and magnitude of the principal stresses for the model in compressible material ($\dot{\epsilon}_1/\dot{\epsilon}_1 = 0.33$) are in agreement with the results of Dieterich & Carter (1969) and Dieterich (1969), whereas the stress distribution in the case of incompressible material properties seems to indicate an unstable situation in the analysis.

In a review of studies of quartz deformation lamellae and calcite twin lamellae fabrics from natural folds (Dieterich & Carter 1969), it was found that the principal stress directions inferred from the fabrics are compatible with the stress directions in the fold models. The inferred direction of principal stress on the limbs of the natural folds is inclined to the layering in the same sense as in the models, but in the natural folds the angle between the principal stress and the layering is consistently smaller. The interpretations were offered in Dieterich & Carter (1969) that the fabrics are controlled by both the relative magnitudes and the orientations of the principal stresses, and that the fabrics are cumulative, having formed during the entire deformation. Later Dieterich (1970) suggested that the stress directions inferred from fabric maxima show the average of the stress directions inferred from fabric maxima show the average of the stress directions for the entire deformation, and that these directions more closely correspond to finite strain axes than to stresses at any given instant in the deformation. Hence, the conclusions imply that scatter in a fabric diagram may reflect the variation of stress orientation with time. These problems need to be studied in more detail, as does the problem of the extent to which the early formed minerals have been rotated during folding. Summarizing the results of distribution of principal stresses, the direction of the compressive stresses lies subparallel to the layer everywhere in the model during the low-amplitude stage of folding. As the fold develops, buckling becomes the dominant mechanism of layer deformation in models with high viscosity contrast. Stretching of the layer on the outside of the fold hinge takes place, and the principal compressive stress (σ_1) becomes oriented normal to the layering. On the limbs of the fold, σ_1 rotates to increasingly larger angles to the layer as the fold grows. For models with a low viscosity contrast the stresses remain nearly parallel to the direction of compression throughout the folding. Stress directions inferred from fabric maxima of folded rocks show the average of the stress directions for the entire deformation, and that these directions are formed by either finite strain or by the magnitude and direction of principal stresses during folding. The application of a nonlinear flow law in the fold model does not significantly alter the stress orientations during the fold history.

DISTRIBUTION OF SHEAR STRESSES AND DEVIATORY STRESSES

Folding implies inhomogeneous strain, and the axes of stress and finite strain do not coincide. As pointed out by Dieterich (1969), this means that, during folding shear stresses act across the surfaces of the axial-plane foliation formed perpendicular to the direction of maximum

compressive strain. Slippage may occur along those for which cleavage has formed, in response to the shear stress.

The distribution of principal deviatoric stresses $\sigma'_1 = \sigma_1 - \bar{\sigma}$ and $\sigma'_2 = \sigma_2 - \bar{\sigma}$, where σ_1 and σ_2 are the principal stresses and $\bar{\sigma}$ the mean stress, are shown in figure 3 for a single-layer fold, with a viscosity contrast of 100/1 between layer and matrix. A layer-parallel pattern of the lines with equal deviatoric stress is shown in the hinge zone. The pattern resembles the distribution of mean stress, but now with opposite sign, Stephansson (1974, fig. 3). In the shear stress, $\tau_{\max} = \frac{1}{2}(\sigma_1 - \sigma_2)$, we note a layer-parallel pattern of the lines of equal shear stress with increasing values towards the surfaces of the folded layer. A singular point, i.e. a point where the two principal stresses are zero, is found at the centre of the layer in the hinge region. These results are different from the stress distribution in a folded layer of gelatin affected by gravity. By using the photo-elastic technique Currie *et al.* (1962) found the highest values of shear stresses in the limb area and at the outer portions of the fold hinge.

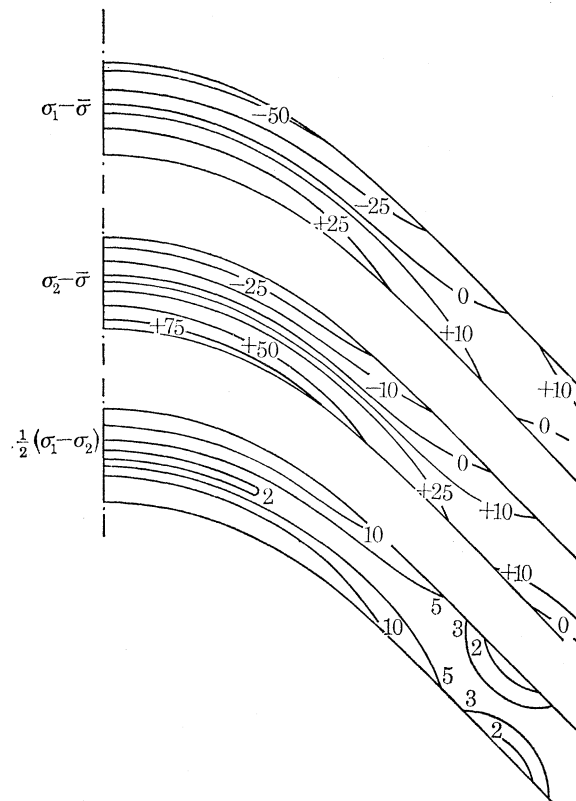


FIGURE 3. Deviatoric stresses (σ'_1 , σ'_2) and maximum shear stress of a competent layer in a single-layer fold with a viscosity contrast of 100/1.

MEAN STRESSES IN FOLDED MODELS

The distribution of the mean stress $\bar{\sigma} = \frac{1}{3}(\sigma_1 + \sigma_2 + \sigma_3)$ for single-layer and multilayer fold structures were studied by Stephansson (1974). Two models were studied for a viscosity contrast between layer and matrix given by the ratio $\mu_1/\mu_2 = 100$, where μ_1 is the viscosity of the layer. One of them, a multilayer model consisting of three competent layers surrounded by incompetent layers and subjected to a small shortening strain rate across the axial surface, is

demonstrated in figure 4. The incompetent layers have twice the thickness of the competent layers and all of them have a fold geometry of similar type.

From the mean stress distribution as shown in figure 4 we note a great difference in the direction of the isopachs (lines of constant mean stress) for the competent layers and the interlayers. The isopachs for the competent layers show a layer-parallel pattern, with the

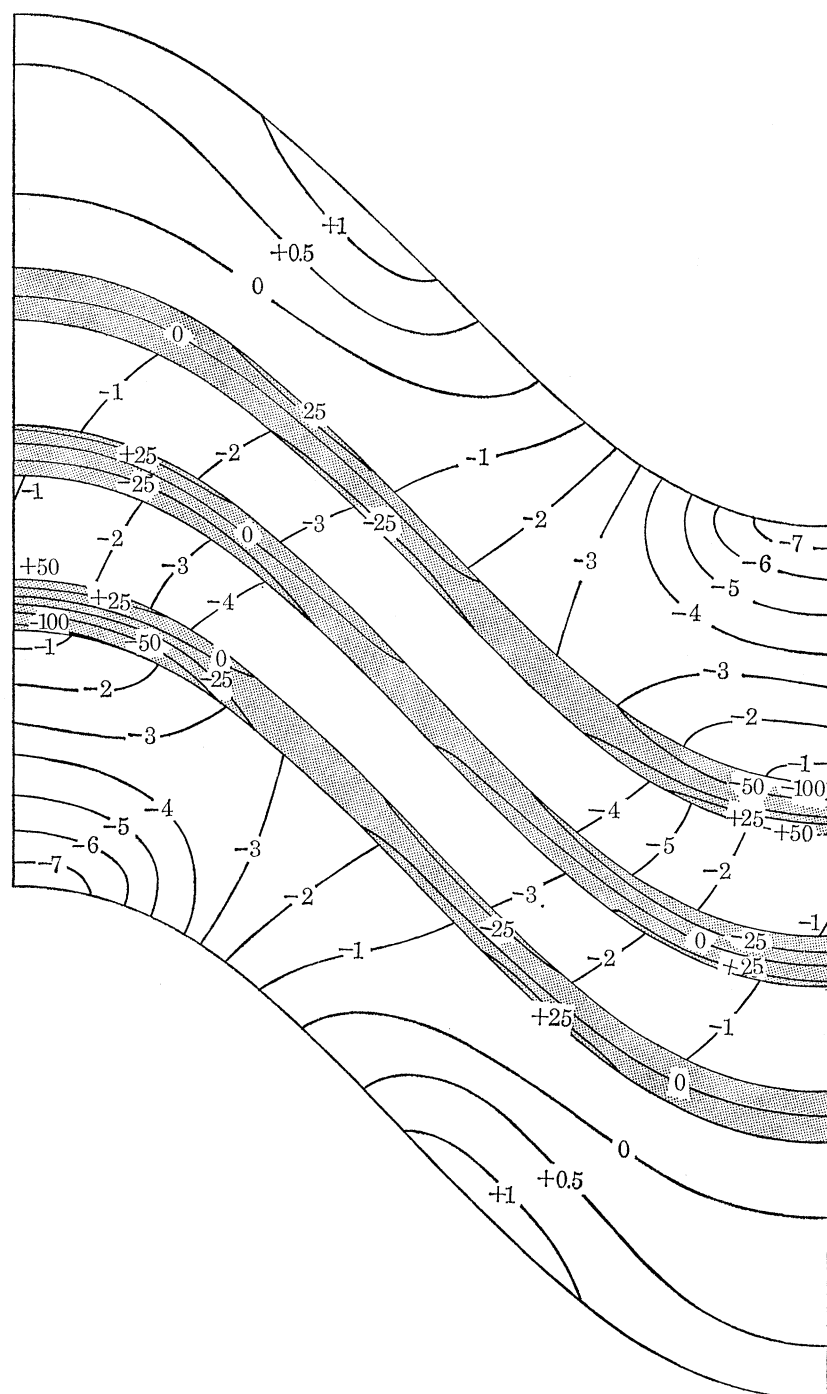


FIGURE 4. Distribution of mean stress in a multilayer model; viscosity contrast of 100/1 between the competent layers (stippled) and the less competent interlayers.

highest value in the similarly folded competent layer of the inner arc of the model. In this study the compressive stresses are by definition negative, and the inner arc of the fold hinge shows the maximum value of the compressive mean stress which also causes a volume increase. The figure indicates that the fold limbs show a moderate compressive mean stress, and that the line of zero mean stress comes nearer the limb of the outer arc layer.

Isopachs of the less competent interlayers are directed almost perpendicular to the layer surfaces, which causes a layer-parallel gradient of the mean stress with lowest value at the hinge zone.

The results in figure 4 show that the mean stress in the innermost folded layer varies from -100 to $+50$ in the hinge zone, i.e. for a folded sequence with the viscosity 10^{21} Pa s (10^{22} P) surrounded by rocks with the viscosity 10^{19} Pa s (10^{20} P) the difference in pressure between the outer and inner arcs would be slightly more than 15 MPa (150 bar). The corresponding pressure difference between the limb and hinge of the incompetent layer is of the order of 0.5 MPa (5 bar.)

Stephansson (1974) studied the mean stress distribution in a fold with a viscosity contrast of 10/1 and deformed to an overall shortening of 60%. In the folded layer all mean stresses are compressive and decreasing along the axial surface from the inner to the outer arc. Here the isopachs are oriented parallel to the direction of compression. The stress pattern in the matrix goes from a minimum value at the outer arc to a maximum in the area of the inflexion point and decreases again towards the inner arc. At a distance in the matrix of about one wavelength from the folded layer, the stresses are uniform and of the same value.

To sum up, for folds with high viscosity ratios the gradient of the mean stress in the hinge part of the competent layer is directed perpendicular to the layer. In the limb zone the mean stress is more uniform and of lower magnitude. The incompetent layers in a folded multilayer sequence show a mean stress gradient parallel to the layer and the pressure minimum is located at the hinge zone. In a folded layer with low viscosity contrast all mean stresses are compressive and decreasing along the axial surface from the inner to the outer arc.

Stephansson (1974) demonstrated that recrystallization of folded rocks under non-hydrostatic stress conditions will result in geochemical mass transport and certain mineral distribution and associations which are related to the mean stress distribution. A heterogeneous stress distribution, such as appears in a fold structure, generates free-energy gradients, and diffusion currents will tend to bring the system to the same state of equilibrium as that which would develop by mechanical-transport processes. The endeavour to achieve equilibrium by lowering the free energy may be related to one or more of the following events: (1) the introduction of new mineral species; (2) a change in the volume of a mineral due to polymorphic phase changes; (3) a change in the chemical composition of individual minerals or co-existing mixed crystals containing the same exchangeable ions; (4) a change in grain size. In the study by Stephansson (1974) the variation in mineral composition bulk chemical composition, chemical composition of a mineral and grain size due to folding were demonstrated with examples taken from the literature.

FUTURE DEVELOPMENT OF THE FINITE ELEMENT ANALYSIS OF FOLDING

The application of the finite element technique has been successful in the study of shape development and stress distribution in a variety of single- and multilayer fold models. For example, the finite deformations which produce large-amplitude folds and the related area of interpretation of fabric elements, e.g. cleavages, lineations and variations of chemical composition in different parts of folds. Future progress is likely to take place along one or more of the following lines: (1) application of recent developments in the finite element technique; (2) more realistic loadings of the models; (3) testing with different flow laws; (4) simulation of rock anisotropies.

As pointed out by Zienkiewicz in this volume, the application of the finite element method in the field geological studies is fairly recent and limited. So far, the structural geologists have been problem-oriented in their studies and many problems remain to be studied with the present technique. The application of three-dimensional finite element models and models with more sophisticated elements and meshes has started.

The finite element technique offers a possibility of a complex loading of the model. So far, simple buckling has been the only loading applied to folding. Development of folds by simple shear or a combination of pure shear and simple shear need to be studied, as does the effect of gravity on fold shape and finite strain and stress distribution. Any of the loadings can be studied with the present techniques.

A nonlinear finite element fold model was presented by Parrish (1973). The result of this study, as well as those of previous linear models, suggests that the application of a single flow law throughout the folding is not sufficient to model most natural rocks. He therefore suggests the application of different flow laws to different parts of the folded layer and matrix.

Simulation of rock anisotropies during the entire history of deformation has not been tested so far. Introduction of different joint elements in the model to simulate cleavage is a possible method. Mineral anisotropy, fabric rotation and plastic flow can easily be modelled with the present technique.

REFERENCES (Stephansson)

- Biot, M. A. 1961 Theory of folding of stratified viscoelastic media and its implication in tectonics and orogenesis. *Geol. Soc. Am. Bull.* **72**, 1595–1620.
- Biot, M. A. 1965 *Mechanics of incremental deformations*. New York: Wiley.
- Chapple, W. M. 1968 A mathematical theory of finite-amplitude rock-folding. *Geol. Soc. Am. Bull.* **79**, 47–68.
- Currie, J. B., Patnode, H. W. & Trump, R. P. 1962 Development of folds in sedimentary strata. *Bull. Geol. Soc. Am.* **73**, 655–674.
- Dieterich, J. H. 1969 Origin of cleavage in folded rocks. *Am. J. Sci.* **267**, 155–165.
- Dieterich, J. 1970 Computer experiments on mechanics of finite amplitude folds. *Can. J. Earth Sci.* **7**, 467–476.
- Dieterich, J. H. & Carter, N. L. 1969 Stress history of folding. *Am. J. Sci.* **267**, 129–154.
- Hudleston, P. J. & Stephansson, O. 1973 Layer shortening and fold-shape development in the buckling of single layers. *Tectonophysics* **17**, 299–321.
- Parrish, D. K. 1973 A non-linear finite element fold model. *Am. J. Sci.* **273**, 318–334.
- Ramberg, H. 1961 Contact strain and folding instability of a multilayered body under compression. *Geol. Rundsch.* **51**, 405–439.
- Ramberg, H. 1964 Selective buckling of composite layers with contrasted rheological properties; a theory for simultaneous formation of several orders of folds. *Tectonophysics* **1**, 307–341.
- Stephansson, O. 1973 The solution of some problems in structural geology by means of the finite element technique. *Geol. Fören. i Stockholm Förh.* **95**, 51–59.
- Stephansson, O. 1974 Stress-induced diffusion during folding. *Tectonophysics* **22**, 233–251.
- Stephansson, O. & Berner, H. 1971 Finite element method in tectonic processes. *Phys. Earth Planet. Inter.* **4**, 301–321.